

Investigation of weld defects and mechanical properties of dissimilar friction stir spot welded dual phase (DP600) steel and aluminum alloy (AA 7075-T6) plates

Ahmet Cakan¹, Mustafa Ugurlu^{2*}

¹ Dept. of Mechanical Engineering, Mersin University, Mersin 33343, Turkey

² Adana Organized Industrial Zone Vocational School of Technical Sciences, Cukurova University, Adana, Turkey

Orcid: A. Cakan (0000-0002-7394-1499), M. Ugurlu (0000-0002-1194-7772)

Abstract: DP600 steel and AA7075-T6 aluminium alloy plates were joined using the friction stir spot welding process. The effects of different tool rotational speeds on the mechanical properties, intermetallic compound formation and interface microstructure of welded joints were investigated. The highest lap shear tensile load was obtained from the samples joined at a rotational speed of 1040 rpm (6.5 kN). It was determined that the tensile load of the welded joint decreased with increasing tool rotational speed. XRD analysis performed on broken surfaces, the intermetallic phase was determined to be $Al_{13}Fe_4$. As a result of Vickers microhardness tests, the samples joined at 1320 rpm and 1500 rpm, in the structure of which intermetallic compounds were determined by XRD analysis, displayed higher hardness values. In addition, when scanning electron microscope images were examined, it was determined that the cracks observed in the samples and the porosity both increased with increasing tool rotational speed.

Keywords: Dissimilar welding, Intermetallic compounds, Mechanical properties, DP600, AA7075-T6.

1. Introduction

Improving passenger safety, reducing fuel consumption, and decreasing carbon emissions are issues of priority for the automotive industry. Although weight reduction is possible by using light materials such as Al alloys, joining different types of materials has come to the fore as a method to provide sufficient strength values. For this reason, the joining of high-strength steel and light aluminium materials became a critical subject for the automotive industry [1,2]. The dissimilar welding of Al and steel materials comes to the fore due to the combination of lightness and high strength properties. However, the application of the traditional resistance spot welding (RSW) process, which is used extensively in the industry [3], is not efficient in dissimilar Al-steel joining. As a result of its very different physical and metallurgical properties, it is prone to the formation of brittle intermetallic compounds. In addition the fusion welded joints of dissimilar materials have welding defects like cavities, porosities, and cracks [4]. Therefore, solid-state welding methods are preferred in joining different types of Materials [5-7]. Friction stir welding (FSW), developed by The Welding Institute (TWI) in 1991, is a solid-state welding

method with low distortion, fewer welding defects, and good mechanical properties, as it is a process that takes place below the melting temperature [8-18]. Using this process, it is possible to successfully join materials with very different properties [19-21]. An application of FSW process to one-point joint is known as friction stir spot welding (FSSW) [22,23]. The FSSW technique, which is a joining method that consists of three stages, was derived from FSW process. After a rotary tool is immersed in overlapping plates at a certain depth, it is allowed to dwell for the specified time and then retracted without horizontal movement [24-26]. FSSW is now recognized as one of the most successful methods for joining of dissimilar metals [27,28]. In addition, due to the advantages of the FSSW method such as low energy requirement and low cost, the FSSW technique has been replacing RSW in the automotive industry [29].

In the FSSW process, despite the relatively low heat input The presence of various intermetallic phases was observed at the weld interface [30]. Hsieh et al. [31] determined that Fe_2Al_5 and Fe_4Al_{13} intermetallic compounds were formed at the interface in the joining of SS400 steel and AA6061 aluminum alloy. Although the parameters of

* Corresponding author.
Email: mugurlu@cu.edu.tr



pin and shoulder diameter, tool rotational speed and dwell time are considered as basic FSSW parameters, the plunge depth of the tool is also considered as an important welding parameter. Haghshenas et al. [32], by plunging the tool into the steel material below, determined that a lower intermetallic layer was formed and the bonding was better. However, materials such as carbides or cubic boron nitride, which are more durable than steel, should be used as tool materials for this method. On the other hand joining can be performed by diffusion without plunging materials into the plate at the bottom [28]. Also the diffusion joint is mostly preferred due to the limited plunging in thin sheets. The method of joining by diffusion has come to the fore as tools require lower strength with the contact of the tool to the softer material at the top, and, as a result, tools produced with less costly material can be used. Fereudini et al. [33] investigated the technique of diffusion bonding using a 2.8-mm-long pin for welding 3-mm-thick Al-5083 and 1 mm thick St-12 sheets. It was determined that the plates joined with rotational speed of 900 rpm had better bond strength than the plates joined with rotational speed of 1100 rpm. In this study, due to the use of thin steel plates and to prevent excessive wear of the tool, diffusion bonding was preferred. Also the effects of various tool rotational speeds (1040 rpm, 1320 rpm, 1500 rpm) on welding defects and mechanical properties in joining AA7075-T6 Al alloy plates with DP600 steel plates using FSSW were investigated.

2. Materials and Methods

Aluminium alloy (AA7075-T6) sheets of $100 \times 30 \times 3$ mm and steel (DP600) sheets of $100 \times 30 \times 1.2$ mm were used for the FSSW process. The experiments were carried out under room conditions, with an overlapping area of $30 \text{ mm} \times 30 \text{ mm}$, with an aluminum plate placed on top of the steel plate. The chemical compositions of AA7075-T6 alloy and DP600 steel were given in Table 1 and Table 2 respectively, mechanical properties of AA7075-T6 alloy and DP600 steel used in the study were given in Table 3. The FSSW of the plates was made using a vertical spindle type 2.8 kW FIRST LC20VGN milling machine. FSSW is a joining method that entails three different stages. After a rotary tool is plunged into plates at a certain depth, it is left to dwell for the specified time and is then retracted without horizontal movement (Fig. 1).

A stirring tool made of hot work tool steel (H13) was used in the FSSW processes. The tool is manufactured with a

shoulder diameter of 20 mm, a conical pin diameter of 4–6 mm and a pin length of 2.8 mm. Fig. 2a shows the schematic diagram of the tool. The plates were joined according to various rotational speeds, namely 1040, 1320, and 1500 rpm. In order to determine the effect of tool rotational speed on welding performance, the dwelling time was kept constant for 10 s and the tool was turned clockwise. The plunging amount of the rotating tool was adjusted by the movement of the milling table in the vertical direction followed by waiting for 10 seconds. The joint performance was determined by conducting metallographic analysis (i.e. scanning electron microscopy, X-ray diffraction analyses), microhardness measurements, and tensile tests. For the preparation of the metallography samples shown in Figure 2d, the wire EDM technique was used. Then samples were sanded with silicon carbide papers of 400, 600, 1200, and 2000 grade and polished with alumina suspensions. Cross sectioned samples were etched with a solution of 2 mL of HF, 3 mL of HCl, and 15 mL of HNO_3 in distilled water for metallographic

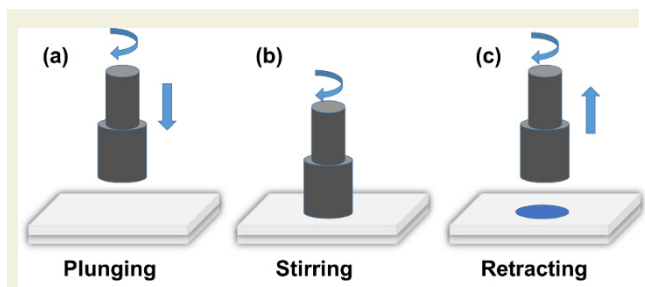


Figure 1. Schematic illustration of the FSSW process (a) plunging stage (b) stirring stage (c) retracting stage.

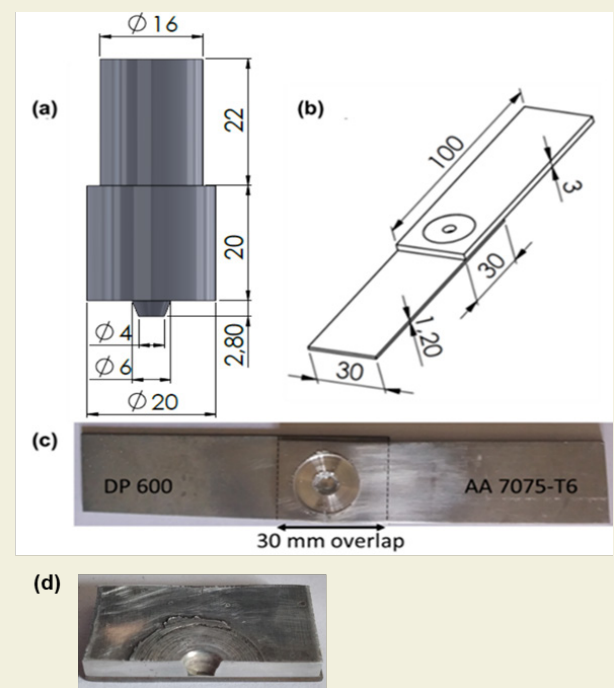


Figure 2. (a) Schematic diagram of the tool used in the FSSW process (b) Dimensions of the friction stir spot welded joint (c) pictorial image of the as welded sample. (d) pictorial image of the metallographic analysis sample

Table 1. Chemical composition of AA7075-T6.

Si	Fe	Cu	Mn	Mg	Cr	Ni	Zn	Ti	Zr	Al
0.07	0.14	1.6	0.06	2.7	0.19	60 ppm	5.8	0.02	0.01	89.4

Table 2. Chemical composition of DP600.

C	Mn	Si	S	Al	P
0.092	1.912	0.147	0.003	0.031	0.014

Table 3. Mechanical properties of the DP600 and AA 7075-T6.

Material	Tensile Strength (MPa)	Yield Strength (MPa)	Elongation Rate (%)	Modulus of Elasticity (GPa)	Hardness (HV)
DP 600	630	370	24	20	170
AA 7075-T6	572	503	11	71	175

analysis (Fig. 2d).

In addition, microhardness measurements were performed on the cross section of the welded plates to determine the hardness changes in the stir zones. For microhardness measurements, Vickers hardness test (Bulut, Microbul) method was used with a load of 100 grams with a loading time of 10 seconds. Fig. 2c and Fig. 2d shows a pictorial image of the as-welded sample that was used for the tensile shear tests and metallographic analyses respectively. For tensile shear test, a minimum of three tensile

specimens for each parameter were tested using a loading speed of 1 mm/min (Fig. 2b).

3. Results and discussion

3.1. Microstructural investigations

The cross-sectional views of Al plates and steel plates joined using different tool rotational speeds are shown in Fig. 3. According to the SEM images, there was no apparent weld defect in the samples joined at 1040 rpm (Fig. 4a) and 1320 rpm (Fig. 4b). In the sample joined at 1500 rpm (Fig. 4c), the presence of cracks in the area below the shoulder was observed. The presence of liquation cracks, whereby cracks occur during the formation of partially melting regions with the heat generated by friction and solidification of those regions, can be seen in Fig. 4c.

Gerlich et al. [34] determined that during the dwell time, reverse flow occurs as a result of the downward force acting on the material under the shoulder of the tool. Yamamoto et al. [35] determined that this reverse flow causes the material to move upwards following the stir zone boundary, and they explained this as the cause of liquation cracks.

It was observed in the SEM images of the region near the pin gap below the shoulder that the sample joined at 1040 rpm (Fig. 4d) did not have significant weld defects, but there were thin cracks in the sample joined at 1320 rpm (Fig. 4e). In addition, the sample joined at 1500 rpm (Fig. 4f) had more prominent and dense cracks, and it was determined that the cracks increased with the tool rotational speed. Since more heat is produced at high tool rotational speed, it is thought that the partially melted regions, which are in higher-temperature liquid form, cause larger cracks during solidification.

When the SEM images of the weld interface according to various tool rotational speeds were examined, it was observed that with the increase of the tool rotational speed, the porosity in the interface microstructure increased (Figs. 5a, 5b, 5c). It was determined that there were small gaps in the microstructure of the sample joined at 1040 rpm, there were dimples and gaps in the sample joined at 1320 rpm, and there were large gaps in the sample joined at 1500 rpm (Figs. 5d, 5e, 5f). This result is thought to have occurred due to the higher heat input when high tool rotational speed was used. Mahto et al. stated that as a result of low heat input, the porosity and intermetallic compound layer formation decreased. However, it was



Figure 3. Cross-sectional views of welded joints according to various tool rotational speeds, (a) 1040 rpm, (b) 1320 rpm, and (c) 1500 rpm.

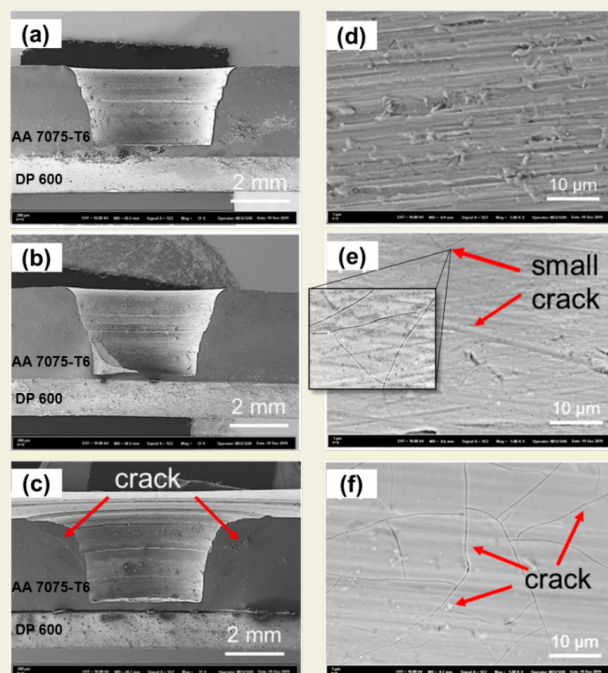


Figure 4. SEM images of welded joints according to various tool rotational speeds, (a-d) 1040 rpm, (b-e) 1320 rpm, and (c-f) 1500 rpm.

stated that due to the high heat input, aluminium softens more than steel, and that leads to an inhomogeneous mixing process and creates porosity in the welding zone [36].

When the cross sectional micrograph of the sample joined at rotational speed of 1040 rpm were examined (Fig. 6d), cracks and cavity-like weld defects were not observed, and a thin intermetallic layer formation was observed at the interface. Also, the crack line and separate zone were observed in samples joined at 1320 rpm and 1500 rpm tool rotational speeds, respectively (Fig. 6e-6f). Sun et al. [27] In their study on the joining of Al and mild steel sheets with FSSW, determined that intermetallic layer formation took place at the Al/Fe interface as a result of the high temperature during the welding process. Esmaili et

al. [37], in their study on joining Al and Cu plates with FSW, determined that when low tool rotational speed is used, the intermetallic layer does not form. They also stated that the intermetallic layer formation begins as the tool rotational speed increases and the thickness of the intermetallic layer increases at a higher tool rotational speed. They concluded that the formation of a thin intermetallic layer increases the tensile strength, whereas the thickening of the intermetallic layer decreases the tensile strength. Bozzi et al. [38], in their study on the joining of Al and steel sheets with FSSW, reported that $FeAl_3$, Fe_2Al_5 , and $FeAl_2$ intermetallic compounds were formed depending on the welding parameters.

When the results of XRD analysis were examined (Fig.

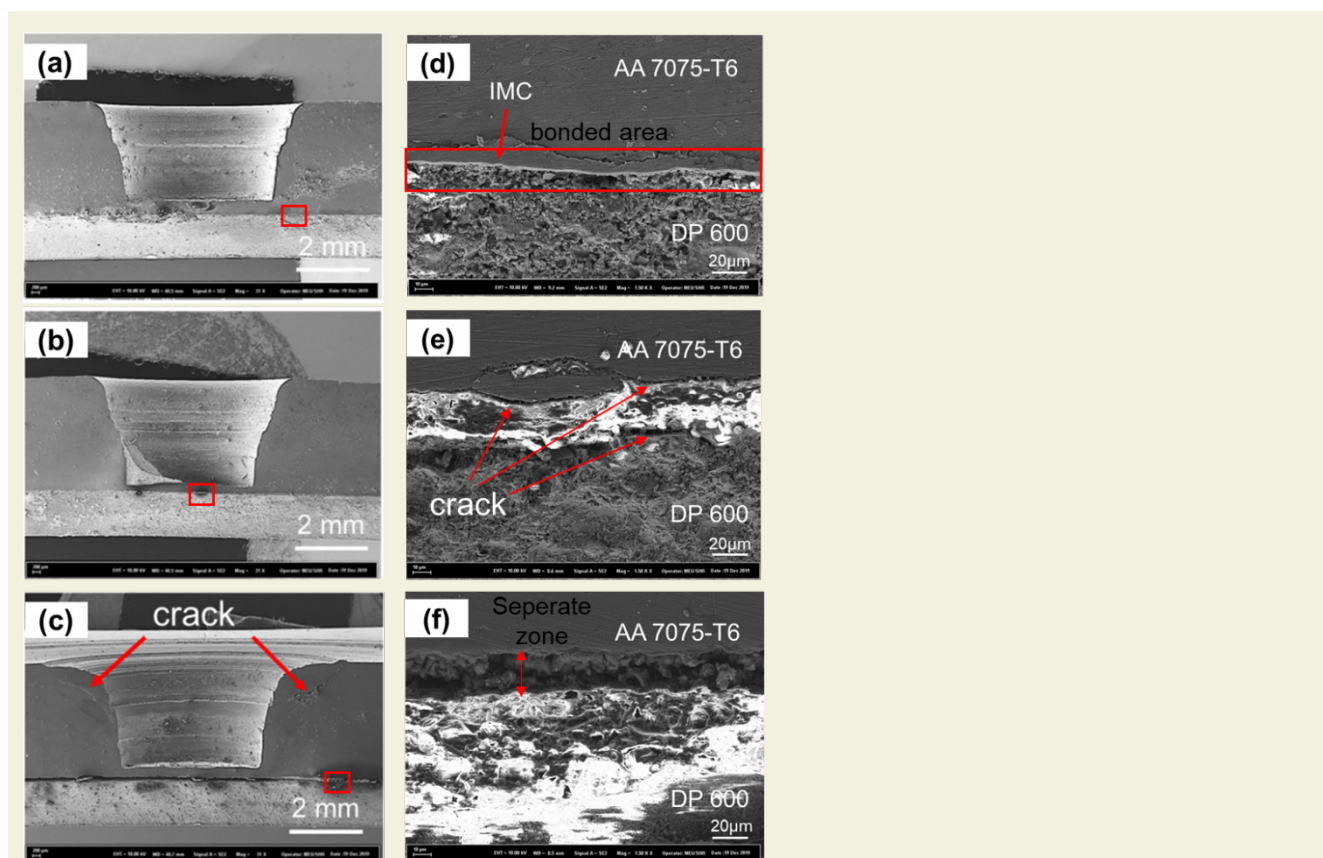


Figure 6. Cross sectional micrograph of samples, (a-d) 1040 rpm, (b-e) 1320 rpm, and (c-f) 1500 rpm.

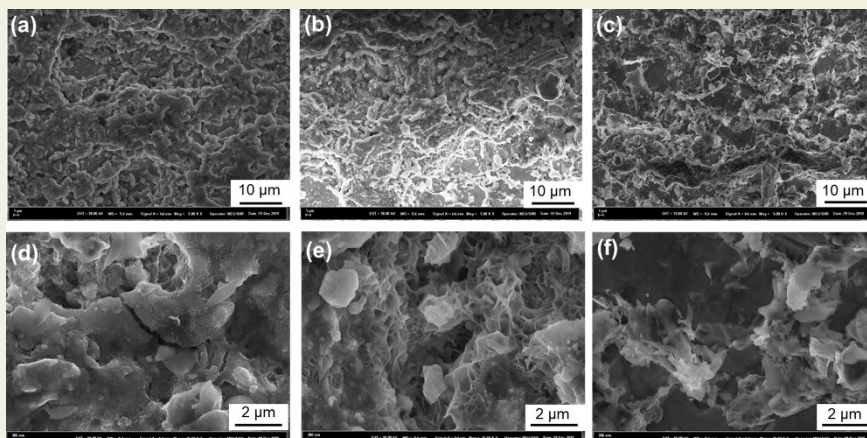


Figure 5. SEM images of weld interface according to various tool rotational speeds, (a-d) 1040 rpm, (b-e) 1320 rpm, and (c-f) 1500 rpm.

7) on the fractured steel sides of the tensile test samples, it was determined that there was mostly an iron phase, in addition to the Al and Zn peaks in the structure, and no apparent intermetallic compound was detected in the sample obtained using 1040 rpm as the tool rotational speed.

When the rotational speed of the tool was chosen as 1320 rpm or 1500 rpm, the presence of peaks similar to those mentioned in the above paragraph was determined. The phases were determined to be mostly Fe and Al, as well as peaks of the $Al_{13}Fe_4$ intermetallic compound.

In studies in the literature on joining pure Al with Zn-coated steel [39], pure Al with low carbon steel [40] and 6063 Al alloy with Zn coated steel [41], it was reported that an $Al_{13}Fe_4$ intermetallic compound was formed. Jiang and Kovacevic [42] reported that Al-Fe intermetallic compounds were formed by reacting with steel as a result of Al melting during the welding process. Lee et al. [43] reported that the first phase that began to nucleate at the Al-Fe interface was the $Al_{13}Fe_4$ phase. As a result of the reaction between $Al_{13}Fe_4$ and Fe, they reported that the Al_5Fe_2 phase occurred, but it was also said that the presence of this structure was not actually detected due

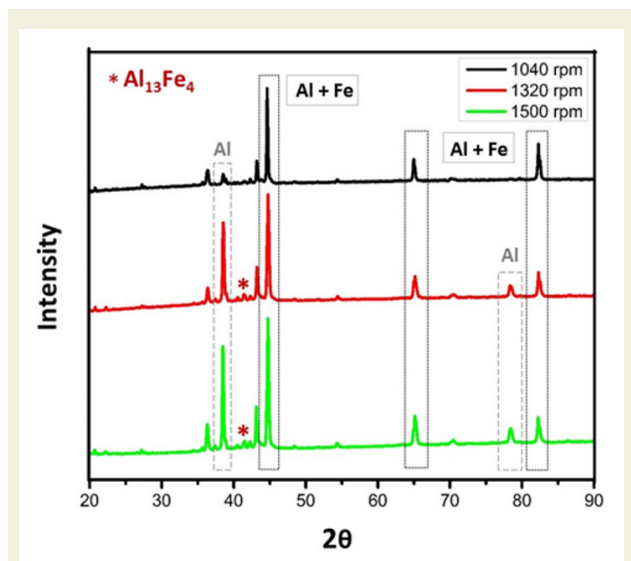


Figure 7. XRD analysis results of shear fracture surface on steel side.

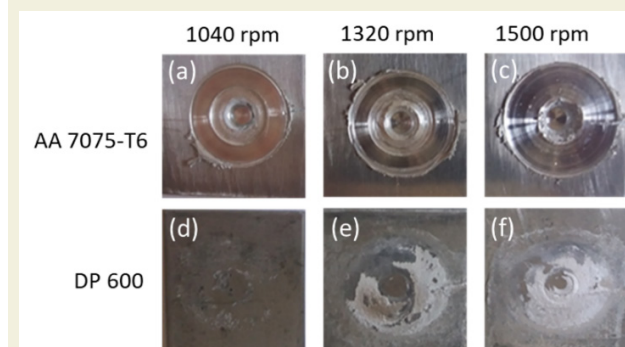


Figure 8. View of stir zones of Al plates (a), (b), (c), and DP600 plates (d), (e), (f) after the tensile test.

to the short dwell time. In the study that we conducted, it was thought that the Al_5Fe_2 phase did not occur due to the joining of the tool without plunging into the steel plate through diffusion. Das et al. [44] reported that the formation of the $Al_{13}Fe_4$ phase increased when a high rotational speed was used, and this was explained by the lower rate of cooling at high rotational speed.

3.2. Tensile shear force

Fig. 8 shows the top surfaces of the DP 600/AA7075-T6 joints obtained under various FSSW process parameters. The materials used during the FSSW process were exposed to friction and downward force by the tool. For this reason, the steel material was transported towards the plasticized aluminum material side. Increasing the temperature in the stir zone (SZ) leads to the transfer of more materials from one to the other in the joined samples due to diffusion. When the surface of the Al plates at the top in the welding process was examined, it was determined that a similar appearance formed for various rotational

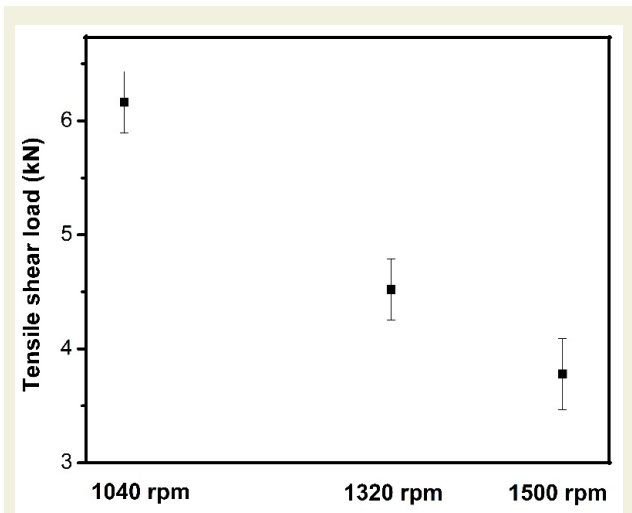


Figure 9. Lap shear fracture load of FSS-welded sheets according to various tool rotational speeds.

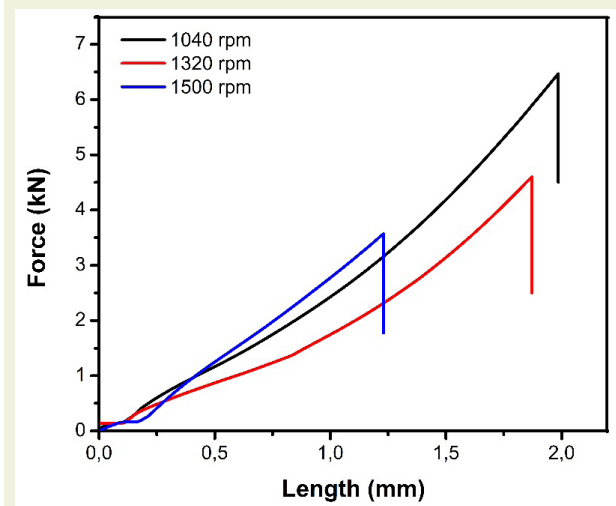


Figure 10. Force-elongation curves of welded joints according to various tool rotational speeds.

speeds (1040, 1320, and 1500 rpm), and, as a result of material transfer, shoulder and pin pits formed.

The fracture load values and force-elongation curves for the welded parts according to various tool rotational speeds are given in Fig. 9 and Fig. 10, respectively. It was determined that there was a decrease in the fracture loads due to the increasing tool rotational speed, and the highest fracture load of 6.5 kN was obtained from the sample joined at the rotational speed of 1040 rpm. The lowest fracture load of 3.5 kN was obtained from the sample joined with rotational speed of 1500 rpm (Fig. 9). The reason for the decrease in the fracture load determined at high tool rotational speed (1500 rpm) is thought to be the fragile intermetallic compounds that formed as a result of increased temperature in the welding zone. Choi et al. [45] reported in their study on the joining of Al and Mg sheets with FSSW that the tensile strength was decreased with the increase of the tool rotational speed. They explained this reduction in tensile strength with the thickness of the layer formed by the reaction and the cracks found.

3.3. Vickers microhardness

Vickers hardness values for each of the joints produced by FSSW at different rotational speeds are given in Fig. 11. The Vickers hardness measurements were carried out on the top plate 1 mm above the overlap line. As seen in Fig. 11, the sample joined with rotational speed of 1040 rpm had lower Vickers hardness values, while the samples joined at 1320 rpm and 1500 rpm showed similar hardness values. This change of hardness values obtained by moving away from the welding centre was similar for various rotational speeds, and with the distance away from the welding centre, the hardness values were first decreased and then increased. It is thought that the decrease in hardness values occurs in the heat-affected zone. Venukumar et al. [46] explained this situation with the coarsening of the grains as a result of excessive aging. A

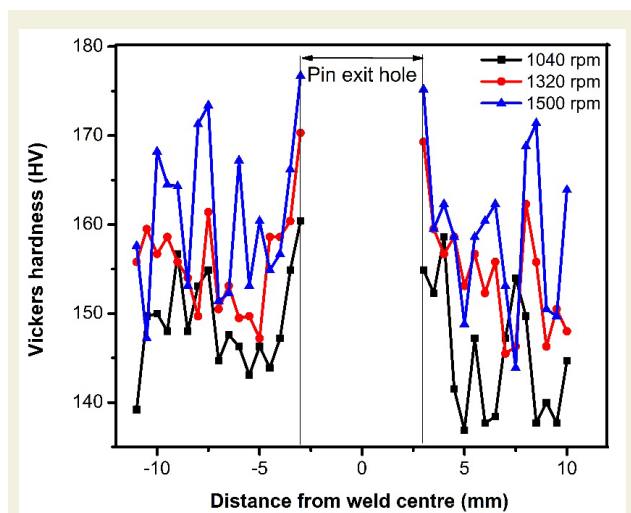


Figure 11. Vickers hardness values of FSW-welded joints using various rotational speeds.

hardness value of approximately 160 HV was obtained for various rotational speeds at the exit hole of the pin. In the heat-affected zone, a hardness value of approximately 140 HV was measured for the sample joined at a rotational speed of 1040 rpm, and similar values for samples joined at rotational speeds of 1320 rpm and 1500 rpm were measured as approximately 150 HV.

4. Conclusions

In this study, DP600 steel and AA 7075-T6 al alloys were welded by FSSW method. The effects of various tool rotational speeds (1040 rpm, 1320 rpm, 1500 rpm) on joint performance were investigated.

The SEM examinations of the dissimilar spot welds fabricated by FSSW using different rotational speeds revealed that the sample joined using rotational speed of 1040 rpm did not exhibit any obvious cracks while cracking in the welding area of the samples joined at 1320 rpm and 1500 rpm was present. It was also determined that the cracking and porosity increased with increasing tool rotational speed. As a result of the XRD analysis of the fractured steel sides after the tensile testing, it was observed that the parts joined at 1320 rpm and 1500 rpm included the intermetallic $Al_{13}Fe_4$ phase. When the Vickers hardness values of the welded samples were compared, it was observed that the samples joined at 1320 rpm and 1500 rpm had hardness values close to each other, with hardness of approximately 150 HV, and the sample joined at 1040 rpm had the lowest hardness with a hardness value of 140 HV. It was determined that there was a decrease in the tensile shear force due to the increase in the tool rotational speed. The lowest tensile shear force was obtained as 3.5 kN from the sample joined at rotational speed of 1500 rpm. The highest tensile shear force was obtained as 6.5 kN from the sample joined using rotational speed of 1040 rpm.

5. References

- [1] Ogura, T., Saito, Y., Nishida, T., Nishida, H., Yoshida, T., Omichi, N., Fujimoto, M., Hirose, A., (2012). Partitioning evaluation of mechanical properties and the interfacial microstructure in a friction stir welded aluminum alloy/stainless steel lap joint, *Scripta Materialia*. 66(8): 531–534. <https://doi.org/10.1016/j.scriptamat.2011.12.035>.
- [2] Ogura, T., Nishida, T., Tanaka, Y., Nishida, H., Yoshikawa, S., Fujimoto, M., Hirose, A., (2013). Microscale evaluation of mechanical properties of friction stir welded A6061 aluminum alloy / 304 stainless steel dissimilar lap joint, *Science and Technology of Welding and Joining*. 18(2): 108–113. <https://doi.org/10.1179/1362171812Y.0000000098>.
- [3] Doruk, E., Pakdil, M., Çam, G., Durgun, İ., Kumru, U. C., (2016). Resistance spot welding applications in automotive industry. *Engineer and Machinery*, 57(673): 48-53.
- [4] Zhang, W., Sun, D., Han, L., Gao, W., Qiu, X., (2011). Characterization of intermetallic compounds in dissimilar material resistance spot welded joint of high strength steel and aluminum alloy. *The Iron and Steel Institute of Japan*. 51(11):

- 1870–1877. <https://doi.org/10.2355/isijinternational.51.1870>.
- [5] Cakan, A., Atmaca, H., Ugurlu, M., (2018). Analysis and joining of Al – Cu plates using friction stir welding technique. *European Mechanical Science*. 2(1): 1–8. <https://doi.org/10.26701/ems.358729>.
- [6] Cakan, A., Ugurlu, M., Kaygusuz, E., (2019). Effect of weld parameters on the microstructure and mechanical properties of dissimilar friction stir joints between pure copper and the aluminum alloy AA7075-T6. *Materials Testing*. 61(2): 142–148. <https://doi.org/10.3139/120.111297>.
- [7] Ugurlu, M., Cakan, A., (2019). The effect of tool rotation speed on mechanical properties of friction stir spot welded (FSSW) AA7075-T6 aluminium alloy. *European Mechanical Science*. 3: 97–101. <https://doi.org/10.26701/ems.520139>.
- [8] Çam, G., Javaheri, V., Heidarzadeh, A. (2022). Advances in FSW and FSSW of dissimilar Al-alloy plates. *Journal of Adhesion Science and Technology*, 1-33. <https://doi.org/10.1080/01694243.2022.2028073>.
- [9] Çam, G., (2011). Friction stir welded structural materials: beyond Al-alloys. *International Materials Reviews*, 56(1): 1-48. <https://doi.org/10.1179/095066010X12777205875750.10>.
- [10] Çam, G., İpekoğlu, G., (2017). Recent developments in joining of aluminum alloys. *The International Journal of Advanced Manufacturing Technology*, 91(5): 1851-1866. <https://doi.org/10.1007/s00170-016-9861-0>. 11
- [11] Çam, G., İpekoğlu, G., Tarık Serindağ, H., (2014). Effects of use of higher strength interlayer and external cooling on properties of friction stir welded AA6061-T6 joints. *Science and Technology of Welding and Joining*, 19(8): 715-720. <https://doi.org/10.1179/1362171814Y.0000000247>.
- [12] Çam, G., Mistikoglu, S., Pakdil, M., (2009). Microstructural and mechanical characterization of friction stir butt joint welded 63% Cu-37% Zn brass plate. *Welding Journal*, 88(11): 225-232.
- [13] Küçükömeroğlu, T., Aktarer, S. M., Çam, G., (2019). Investigation of mechanical and microstructural properties of friction stir welded dual phase (DP) steel. In *IOP Conference Series: Materials Science and Engineering*. 629(1): 012010. <https://doi.org/10.1088/1757-899X/629/1/012010>.
- [14] Küçükömeroğlu, T., Aktarer, S. M., İpekoğlu, G., Çam, G., (2018). Mechanical properties of friction stir welded St 37 and St 44 steel joints. *Materials Testing*. 60(12): 1163-1170. <https://doi.org/10.3139/120.111266>.
- [15] İpekoğlu, G., Erim, S., Kırıl, B. G., Çam, G., (2013). Investigation into the effect of temper condition on friction stir weldability of AA6061 Al-alloy plates. *Kovove Materialy*, 51(3): 155-163. <https://doi.org/10.4149/km-2013-3-155>. 16.
- [16] İpekoğlu, G., Çam, G., (2014). Effects of initial temper condition and postweld heat treatment on the properties of dissimilar friction-stir-welded joints between AA7075 and AA6061 aluminum alloys. *Metallurgical and Materials Transactions A*, 45(7): 3074-3087.
- [17] İpekoğlu, G., Çam, G., (2012). The effect of temper condition on friction stir welding of dissimilar Al-alloys (AA6061/AA7075) plates. *Engineer and Machinery*, 53(629): 40-47.
- [18] İpekoğlu, G., Gören Kırıl, B., Erim, S., Çam, G., (2012). Investigation of the effect of temper condition on friction stir weldability of AA7075 Al-alloy plates. *Materials Technology*, 46(6): 627-632. <https://doi.org/669.715:621.791:620.17>.
- [19] Çam, G., (2005). Friction stir welding: A novel welding technique developed for Al-alloys. *Engineer and Machinery*. 46(541): 30-39.
- [20] Cam, G., Gucluer, S., Cakan, A., Serindag, H.T., (2009). Mechanical properties of friction stir butt-welded Al-5086 H32 plate, *Materwissenschaft und Werkstofftechnik: Entwicklung, Fertigung, Prüfung, Eigenschaften und Anwendungen Technischer Werkstoffe*. 40: 638–642. <https://doi.org/10.1002/mawe.200800455>.
- [21] Mahto, R.P., Kumar, R., Pal, S.K., (2020). Characterizations of weld defects, intermetallic compounds and mechanical properties of friction stir lap welded dissimilar alloys, *Materials Characterization*. 160: 110115. <https://doi.org/10.1016/j.matchar.2019.110115>.
- [22] Schneider, J., Radzilowski, R., (2014). Welding of very dissimilar materials (Fe-Al), *Jom*. 66(10): 2123–2129. <https://doi.org/10.1007/s11837-014-1134-5>.
- [23] Bozkurt, Y., Salman, S., Çam, G., (2013). Effect of welding parameters on lap shear tensile properties of dissimilar friction stir spot welded AA 5754-H22/2024-T3 joints. *Science and Technology of Welding and Joining*. 18(4): 337-345. <https://doi.org/10.1179/1362171813Y-0000000111>.
- [24] Ibrahim, H.K., Khuder, A.W.H., Muhammed, M.A.S., (2019). Effect of tool-pin geometry on microstructure and temperature distribution in friction stir spot welds of similar AA2024-T3 aluminum alloys. *International Journal of Mechanical and Mechatronics Engineering*. 19: 14–28.
- [25] Shen, Z., Ding, Y., Gerlich, A.P., (2019). Advances in friction stir spot welding, *Critical Reviews in Solid State Materials Sciences*. 8436. <https://doi.org/10.1080/10408436.2019.1671799>.
- [26] Li, M., Zhang, C., Wang, D., Zhou, L., Wellmann, D., Tian, Y., (2020). Friction stir spot welding of aluminum and copper: A review, *Materials*. 13(1): 156. <https://doi.org/10.3390/ma13010156>.
- [27] Sun, Y.F., Fujii, H., Takaki, N., Okitsu, Y., (2013). Microstructure and mechanical properties of dissimilar Al alloy/steel joints prepared by a flat spot friction stir welding technique. *Materials and Design*. 47: 350–357. <https://doi.org/10.1016/j.matdes.2012.12.007>.
- [28] Piccini, J.M., Svoboda, H.G., (2017). Tool geometry optimization in friction stir spot welding of Al-steel joints. *Journal of Manufacturing Processes*. 26: 142–154. <https://doi.org/10.1016/j.jmappro.2017.02.004>.
- [29] Sun, Y., Fujii, H., Zhu, S., Guan, S., (2019). Flat friction stir spot welding of three 6061-T6 aluminum sheets. *Journal of Materials Processing Technology*. 264: 414–421. <https://doi.org/10.1016/j.jmatprotec.2018.09.031>.
- [30] Wang, T., Sidhar, H., Mishra, R.S., Hovanski, Y., Upadhyah, P., Carlson, B., (2019). Evaluation of intermetallic compound layer at aluminum steel interface joined by friction stir scribe technology. *Materials and Design*. 174: 1–6. <https://doi.org/10.1016/j.matdes.2019.107795>.
- [31] Hsieh, M.J., Lee, R.T., Chiou, Y.C., (2017). Friction stir spot fusion welding of low carbon steel to aluminium alloy. *Journal of Materials Processing Technology*. 240: 118–125. <https://doi.org/10.1016/j.matprotec.2016.08.034>.
- [32] Haghshenas, M., Abdel-Gwad, A., Omran, A.M., Gokce, B., Sahraeinejad, S., Gerlich, A.P., (2014). Friction stir weld assisted diffusion bonding of 5754 aluminum alloy to coated high

- strength steels. *Materials and Design*. 55: 442–449. <https://doi.org/10.1016/j.matdes.2013.10.013>.
- [33] Fereiduni, E., Movahedi, M., Kokabi, A.H., (2015). Aluminum/steel joints made by an alternative friction stir spot welding process. *Journal of Materials Processing Technology*. 224: 1–10. <https://doi.org/10.1016/j.jmatprotec.2015.04.028>.
- [34] Su, P., Gerlich, A., North, T.H., Bendzsak, G.J., (2007). Inter-mixing in dissimilar friction stir spot welds. *Metallurgical and Materials Transactions A*. 38: 584–595. <https://doi.org/10.1007/s11661-006-9067-4>.
- [35] Yamamoto, M., Gerlich, A., North, T.H., Shinozaki, K., (2008). Cracking in dissimilar Mg alloy friction stir spot welds. *Science and Technology of Welding and Joining*. 13(7): 583–592. <https://doi.org/10.1179/174329308X349520>.
- [36] Mahto, R.P., Gupta, C., Kinjawadekar, M., Meena, A., Pal, S.K., (2019). Weldability of AA6061-T6 and AISI 304 by underwater friction stir welding. *Journal of Manufacturing Processes*. 38: 370–386. <https://doi.org/10.1016/j.jmapro.2019.01.028>.
- [37] Esmaeili, A., Zareie Rajani, H.R., Sharbati, M., Givi, M.K.B., Shamanian, M., (2011). The role of rotation speed on intermetallic compounds formation and mechanical behavior of friction stir welded brass/aluminum 1050 couple. *Intermetallics*. 19(11): 1711–1719. <https://doi.org/10.1016/j.intermet.2011.07.006>.
- [38] Bozzi, S., Helbert-Etter, A.L., Baudin, T., Criqui, B., Kerbiguet, J.G., (2010). Intermetallic compounds in Al 6016/IF-steel friction stir spot welds. *Materials Science and Engineering: A*. 527(16-17): 4505–4509. <https://doi.org/10.1016/j.msea.2010.03.097>.
- [39] Ahmed, E., Makoto, T., Kenji, I., (2005). Friction stir welded lap joint of aluminum to zinc coated steel. *Quarterly Journal of the Japan Welding Society*. 23(2): 186–193. <https://doi.org/10.2207/qjws.23.186>.
- [40] Elrefaey, A., Gouda, M., Takahashi, M., Ikeuchi, K., (2005). Characterization of aluminum/steel lap joint by friction stir welding. *Journal of Materials Engineering and Performance*. 14(1): 10–17. <https://doi.org/10.1361/10599490522310>.
- [41] Das, H., Basak, S., Das, G., Pal, T.K., (2013). Influence of energy induced from processing parameters on the mechanical properties of friction stir welded lap joint of aluminum to coated steel sheet. *The International Journal of Advanced Manufacturing Technology*. 64(9): 1653–1661. <https://doi.org/10.1007/s00170-012-4130-3>.
- [42] Jiang, W.H., Kovacevic, R., (2004). Feasibility study of friction stir welding of 6061-T6 aluminium alloy with AISI 1018 steel. *Proceedings of the Institution of Mechanical Engineers, Part B: Journal of Engineering Manufacture*. 218(10): 1323–1331. <https://doi.org/10.1243/0954405042323612>.
- [43] Lee, I.S., Kao, P.W., Ho, N.J., (2008). Microstructure and mechanical properties of Al–Fe in situ nanocomposite produced by friction stir processing. *Intermetallics*. 16(9): 1104–1108. <https://doi.org/10.1016/j.intermet.2008.06.017>.
- [44] Das, H., Jana, S.S., Pal, T.K., De, A., (2014). Numerical and experimental investigation on friction stir lap welding of aluminium to steel. *Science and Technology of Welding and Joining*. 19(1): 69–75. <https://doi.org/10.1179/1362171813Y.0000000166>.
- [45] Choi, D.H., Ahn, B.W., Lee, C.Y., Yeon, Y.M., Song, K., Jung, S.B., (2011). Formation of intermetallic compounds in Al and Mg alloy interface during friction stir spot welding. *Intermetallics*. 19(2): 125–130. <https://doi.org/10.1016/j.intermet.2010.08.030>.
- [46] Venkumar, S., Yalagi, S., Muthukumar, S., (2013). Comparison of microstructure and mechanical properties of conventional and refilled friction stir spot welds in AA 6061-T6 using filler plate. *Transactions of Nonferrous Metals Society of China*. 23(10): 2833–2842. [https://doi.org/10.1016/S1003-6326\(13\)62804-6](https://doi.org/10.1016/S1003-6326(13)62804-6).